ORTHOPAEDIC SURGERY

A novel model to study metaphyseal bone healing under defined biomechanical conditions

Lutz Claes · Andreas Veeser · Melanie Göckelmann ·
Ulrich Simon · Anita Ignatius

Abstract

Introduction Experimental studies on metaphyseal fractures are rare and do not control the biomechanical conditions in the healing zone. This study aimed to develop an improved experimental model, which characterizes and controls the biomechanical condition in the fracture gap of a metaphyseal fracture.

Materials and methods A partial osteotomy model in the distal femur of the sheep was developed. The osteotomy was located in the region of the trochlea groove. The osteotomy gap was 3 mm wide. The retro-patellar force acting on the joint in vivo causes a bending of the trochlea resulting in a narrowing of the osteotomy gap. To limit and control this interfragmentary movement, stainless steel plates of various thicknesses were implanted into the osteotomy gap. Forces acting on the trochlea were analyzed and a load-deflection curve of the model was determined in vitro. A pilot study on two sheep was performed using the new model with two different interfragmentary movements of 0.3 or 1 mm. Eight weeks, post-operatively, the sheep were sacrificed and undecalcified histology was performed.

Results The biomechanical analysis of the joint forces and the in vitro load-deflection behavior of the trochlea revealed that the forces acting on the trochlea were high enough to cause an interfragmentary movement of 1 mm in the osteotomy gap. This was confirmed by an X-ray of the sheep, which showed a closing of the proximal osteotomy gap under weight-bearing conditions. The histological section revealed no external callus formation. The sheep with the 0.3 mm interfragmentary movement showed almost complete bridging of the osteotomy gap with woven bone whereas the sheep with the 1 mm interfragmentary movement exhibited new bone formation only at the borderline of the osteotomy but larger areas with connective tissue or even fibrous cartilage in the center of the gap.

Conclusion This metaphyseal bone-healing model provides defined and adjustable biomechanical conditions. The histological images demonstrated intramembranous and endochondral bone healing in the osteotomy gap without callus formation. The model therefore seems appropriate to study metaphyseal bone healing under differing mechanical conditions.

Keywords Fracture healing · Bone · Histology · Experimental model · Biomechanics

Introduction

Fracture healing in cancellous bone is of great importance due to the large number of metaphyseal fractures, which are associated with the elderly population and the associated increasing incidence of osteoporosis. In spite of the rising clinical problem of metaphyseal fractures, most of the experimental studies on fracture healing have been performed on the cortical bone shaft. However, due to the different structure of cortical and cancellous bone, it is assumed that the bone-healing process might differ in compact and trabecular bone and this is actually confirmed by the few experimental studies, which have so far been performed in the metaphysis. In these studies osteotomy

L. Claes (✉) · A. Veeser · M. Göckelmann · U. Simon ·
A. Ignatius
Institute of Orthopaedic Research an Biomechanics,
University of Ulm, Helmholtzstraße 14,
89081 Ulm, Germany
e-mail: lutz.claes@uni-ulm.de

models at the distal femur of rats [12], rabbits [12], or dogs [12] were used. In the main, it was demonstrated that the pattern of fracture healing in the metaphysis differed from that of shaft fractures and occurred without the formation of a pronounced callus formation [12].

However, the experimental models used in these studies have some limitations; the most important being the non-standardized biomechanical conditions. It is well-known that the interfragmentary movement induced by the load acting on the fracture and the stability of the fracture fix-ation is one of the major factors, which guide the healing process of shaft fractures [2–5, 8, 10]. It is very likely that the biomechanical conditions are also crucial in metaphy-seal fracture healing and have, therefore, to be necessarily respected in experimental models. In fact, some of the above-mentioned authors investigated the influence of the mechanical conditions on metaphyseal fracture healing by comparing stable and unstable fracture situations [9]. The authors found direct trabecular bone healing under stable conditions and fibrous tissue under unstable conditions. However, the biomechanical conditions were not defined or controlled and the histological outcome could, therefore, not be correlated to the interfragmentary movement in the healing zone.

There is still an urgent need for a standardized model to test possible therapeutic strategies for the improvement of metaphyseal fracture healing under defined biomechanical conditions. This study aimed to develop an improved experimental model for the investigation of metaphyseal fracture healing, to test the biomechanical conditions in vitro and also the applicability in vivo in a pilot experiment on sheep.

Materials and methods

Development of the model

A standardized fracture was simulated by a partial osteot-omy in the distal femur in sheep (Fig. 1). The osteotomy was located in the region of the trochlea groove and was oriented from the proximal end of the trochlea to the junction of the distal trochlea and the femoral condyles. At the distal end, a bony bridge of 15 mm was kept (Figs. 1, 3). The osteotomy gap was 3 mm wide. The resultant retro-patellar force caused a bending of the trochlea resulting in a narrowing of the osteotomy gap. To limit and control this interfragmentary movement, a small stainless steel plate was implanted into the proximal end of the osteotomy gap (Figs. 1, 4b). Using plates of various thicknesses, the in-terfragmentary movement could be limited to different levels. Thus different mechanical conditions for bone-healing conditions could be created.
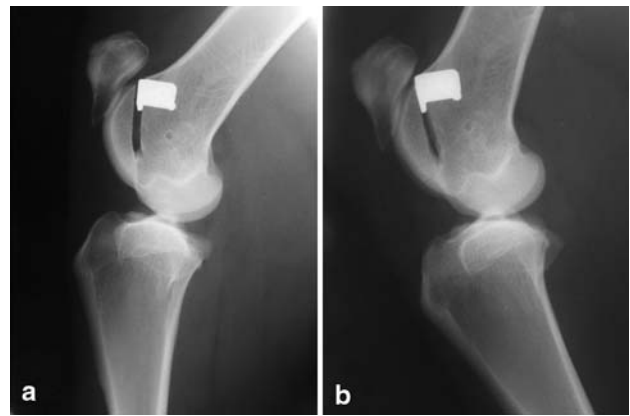
Fig. 1 X-ray of the sheep knee with a partial osteotomy and an implant, which limits the deflection of the osteotomy gap under loading of the extremity. **a** in an unloaded situation, **b** under load and closing of the most proximal osteotomy gap

Calculation of the retro-patellar forces

In vivo patella forces were calculated and applied to an in vitro model in a material testing machine to prove that physiological patella loads lead to bending of the trochlea of a sufficiently high level to create sufficient movement at the osteotomy gap. The calculation of the forces was based on the following biomechanical assumptions for the flexed knee joint in standing position: the flexing moment of the hip resultant force ($F_H \times L_H$) must be counteracted by the knee extensors (Fig. 2). The main knee extensors are the patellar tendon force F_{PT} acting on the lever arm L_{PT} and the force of the long digital extensor muscle F_{DL} acting on the lever arm L_{DL}. This leads to the following equation:

$$F_H L_H = F_{PT} L_{PT} + F_{DL} L_{DL}$$

From the literature, it is known that in sheep the ratio between the muscle cross-section of the long digital extensor muscle and the quadriceps muscle is approximately 1:4 [6]. Assuming that the muscle forces are proportional to their cross-sections we obtained:

$$F_H L_H = F_{PT} L_{PT} + 0.25\, F_{PT} L_{DL} = F_{PT}(L_{PT} + 0.25\, L_{DL})$$

The lever arms are mainly a function of the flexion angle between femur and tibia. For a standing position, this angle is about 125° and the lever arm L_H is about 55 mm. The lever arms obtained from X-rays and measurements on sheep cadaver legs of the muscle forces are approximately:

$$L_{PT} = 35\,\text{mm} \quad \text{and} \quad L_{DL} = 16\,\text{mm}$$

The resultant hip force for a 70 kg sheep was assumed to be $F_H = 875$ N (125% body weight, [1]). With this data the force acting in the patella tendon F_{PT} was calculated:
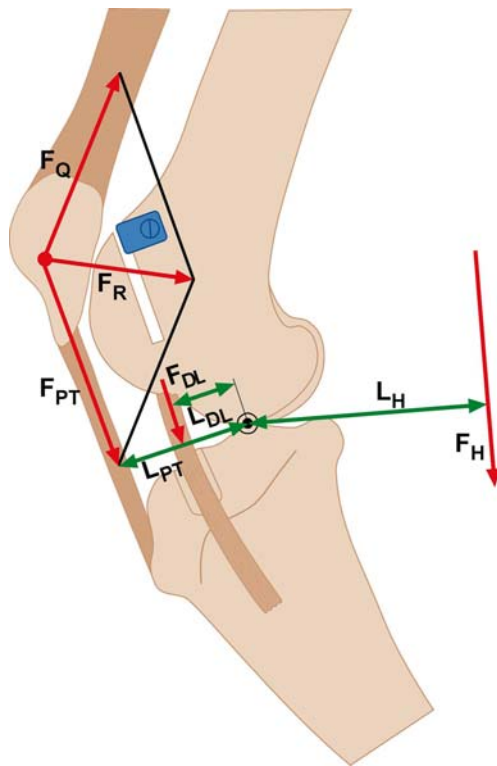
Fig. 2 Forces and lever arms at the sheep knee

$$F_{PT} = F_H L_H / (L_{PT} + 0.25\, L_{DL}) = 1,234\, \text{N}$$

Estimating the direction of the quadriceps force and assuming the resultant patella force acting perpendicular to the contact area between patella and trochlea (Fig. 2) results in a theoretical contact force of 826 N. For higher-knee flexion angles, this force would increase.

Determination of the osteotomy deflection

To determine the load-deflection behavior of the partial osteotomy an in vitro test of an operated distal femur was performed. A partial osteotomy was performed in the right distal femur of a sheep as described later. The bone was fixed in a material testing machine (Z010, Zwick, Ulm, Germany) after embedding with methylmethacrylate (PMMA). A PMMA plug replaced the patella (Fig. 3). A compression force was applied through the PMMA-patella at a direction of 60° to the osteotomy line (Fig. 3). The embedded distal femur was placed on a ball-bearing system, which allowed free movement of the femur perpendicular to the loading axis (Fig. 3). The load to the PMMA-patella was transferred through a ball allowing the application of a pure compression force. The compression force was applied at a rate of 1 mm/min and the force-deflection diagram was recorded.
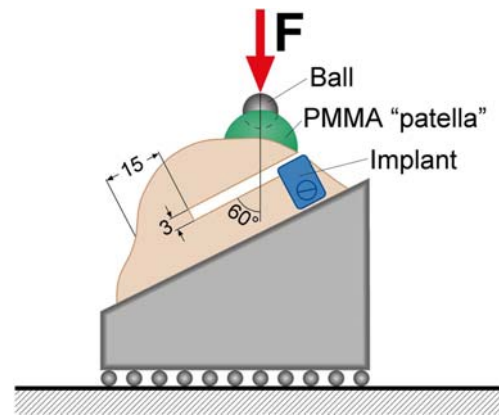

Fig. 3 In vitro testing of the osteotomy deflection under patella compression force

Animal experiment

A pilot study was performed on two sheep (mountain sheep, 58 and 60 kg, 6 years). The animal experiment was conducted following national regulations for the care and use of laboratory animals and approved by the German Government (Regierungspräsidium Tuebingen, No. 875). Surgery was performed under general isoflurane anesthesia (Baxter AG, Voketswil, Switzerland) and premedication with thiopental (Trapanal, Byk Gulden, Netherlands). The right knee joint was opened at the medial side and the patella was dislocated to the lateral side. A custom-made guiding device was temporarily fixed at the medial aspect of the distal femur (Fig. 4a). The guiding device was adjusted to create the osteotomy between the proximal end of the trochlea and the junction of the distal trochlea and the femoral condyle. Subsequently, a 3.2 mm hole was drilled at a distance of 15 mm from the junction between the distal trochlea and the femoral condyle in order to mark the distal end of the osteotomy. Finally the 3 mm osteotomy gap was created by two parallel cuts with an oscillating saw starting proximally and ending at the marking hole. The guiding device allowed a precise orientation of the saw (Fig. 4a). After sawing the resulting bone slice between the two cuts and the guiding device was removed.

To limit the deflection of the osteotomy gap under load, a small distance plate (stainless steel) was placed in the gap at its proximal end and fixed with a screw outside the gap at the medial side of the femur (Fig. 4b). The distance plate devices had various thicknesses. A plate with a thickness of 2.7 mm allowing a maximum deflection of 0.3 mm at the proximal end of the osteotomy was implanted in one sheep. In the second sheep a distance plate device of 2 mm thickness was used allowing a deflection of 1 mm. The patella was relocated and the wound was closed.
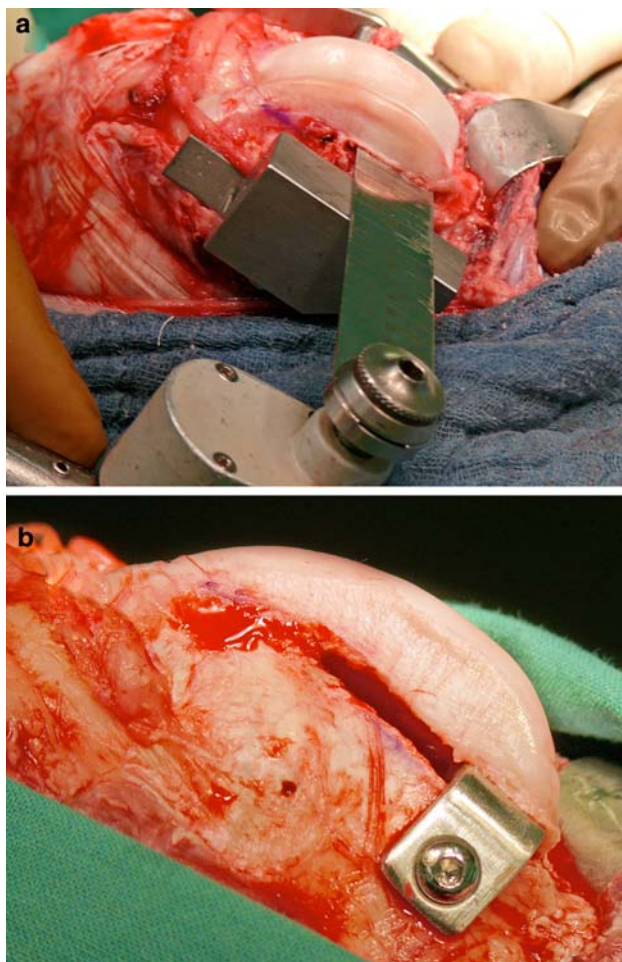
Fig. 4 Intraoperative situs of the opened sheep knee joint; **a** saw guide and oscillating saw to perform two parallel osteotomies, **b** 3 mm wide osteotomy gap with a 2.7 mm angle plate implant for the limitation of the osteotomy gap movement

Immediately after the operation, the animals were allowed freedom of movement. Antibiotics (Amoxicillin 150 mg/10 kg weight, WDT, Garbsen, Germany) and drugs to relieve pain (Rimadyl, Pfizer, Karlsruhe, Germany 4 mg/kg) were administered during the first three postoperative days. Conventional X-rays of the unloaded leg (non weight bearing sheep) were obtained immediately after surgery and again after 4 weeks. An additional X-ray from a loaded leg (standing sheep) was taken 7 days after operation (Fig. 1b).

After 8 weeks, the animals were euthanized and the distal femur was harvested by cutting the femoral shaft at the proximal end of the trochlea. The plates were removed and two parallel cuts performed in the sagittal plane keeping the central section of the distal femur for histological investigation. Undecalcified histological sections were prepared from these bone specimens with a thickness

of 70 μm and surface stained (5 μm) with Paragon (toluidin blue and fuchsin).

Results

Biomechanical considerations

The load-deflection curve showed a linear behavior. The linear part of the curve represents the bending stiffness of the trochlea above the osteotomy gap. This stiffness was 500 N/mm (in direction of the applied load F, Fig. 3). To narrow the osteotomy gap at the most proximal part of the trochlea from 3 to 2 mm (perpendicular to the osteotomy line) a deflection of 1.15 mm in direction of F is necessary (geometrical calculation: 1 mm/sin 60°). A deflection of 1.15 mm corresponds to a force of 575 N in the measured load-deflection plot.

Animal experiment

The animals tolerated the operation well and gross observation revealed return to normal activity and weight bearing after 3 days. X-rays under weight-bearing conditions with the 2 mm implant demonstrated a closing of the osteotomy gap at the location of the implant (Fig. 1b). Only little bone formation was visible after 4 weeks. Eight weeks post-operatively, the X-rays showed new bone formation in the osteotomy gap of both sheep. However, there was more dense bone visible in the sheep with the 2.7 mm plate and the 0.3 mm interfragmentary movement compared to the sheep with the 2 mm plate and the 1 mm interfragmentary movement.

Histology

There was no external callus visible on the medial or lateral side of the knee joint. The osteotomy gap of the sheep with 0.3 mm interfragmentary movement showed a nearly complete filling of the osteotomy gap with trabecular and woven bone (Fig. 5a). The bone formation seemed to be mostly by intramembranous formation with some areas where endochondral ossification could have taken place before (Fig. 6a). The old bone trabeculae showed layers of osteoid and new bone formation (Fig. 6a). The osteotomy gap of the sheep with 1 mm interfragmentary movement showed at the former osteotomy surfaces new bone formation. However large areas of the gap were not filled by bone but connective tissue or even fibrous cartilage (Fig. 5b). Whereas the fibrous cartilage dominated at the area of the largest osteotomy movement, closest to the implant, the connective tissue was mainly located at the
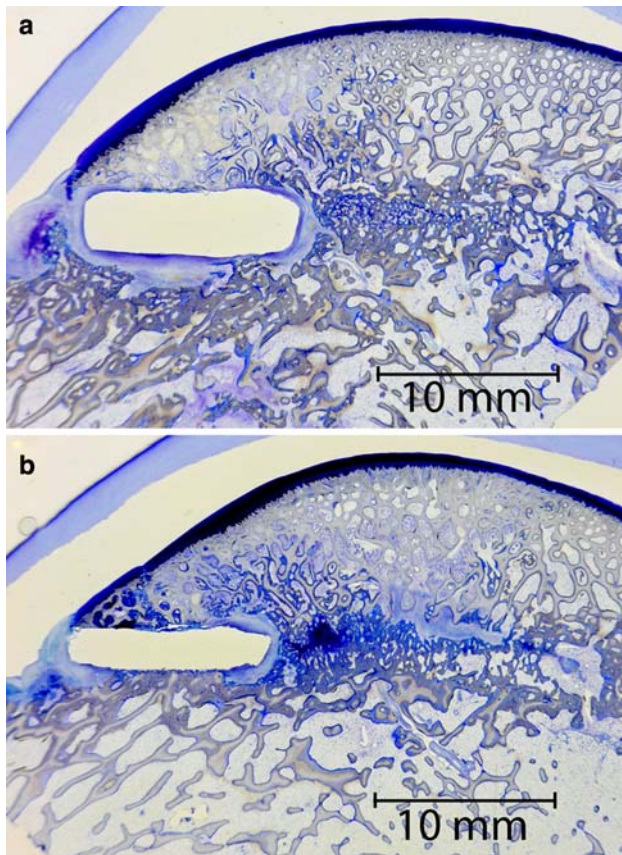
Fig. 5 Undecalcified histological sections through the center of the distal femur (sagittal plan, magnification three times). The *white space* is indicating the location of the removed plate. The 3 mm osteotomy is located in *right hand* of the *white space*. **a** Sheep with 2.7 mm plate, **b** Sheep with 2.0 mm plate

end of the partial osteotomy where the interfragmentary movement is smaller (Figs. 5b, 6b).

Discussion

To our knowledge, the presented model allows to study fracture healing in metaphyseal bone under well-defined biomechanical conditions for the first time. The partial osteotomy is a simplified model of a metaphyseal fracture. All trials with real fractures in metaphyseal bone failed to achieve standardized fracture geometry and were not capable of providing a biomechanically defined and standardized flexible fixation [9]. In the current study a partial osteotomy was chosen because it is difficult to define the biomechanical conditions of a free metaphyseal bone fragment. In order to achieve a defined movement in the osteotomy gap a reversible deflection of the trochlea is prerequisite. This was demonstrated by both in vitro tests and theoretical calculations.

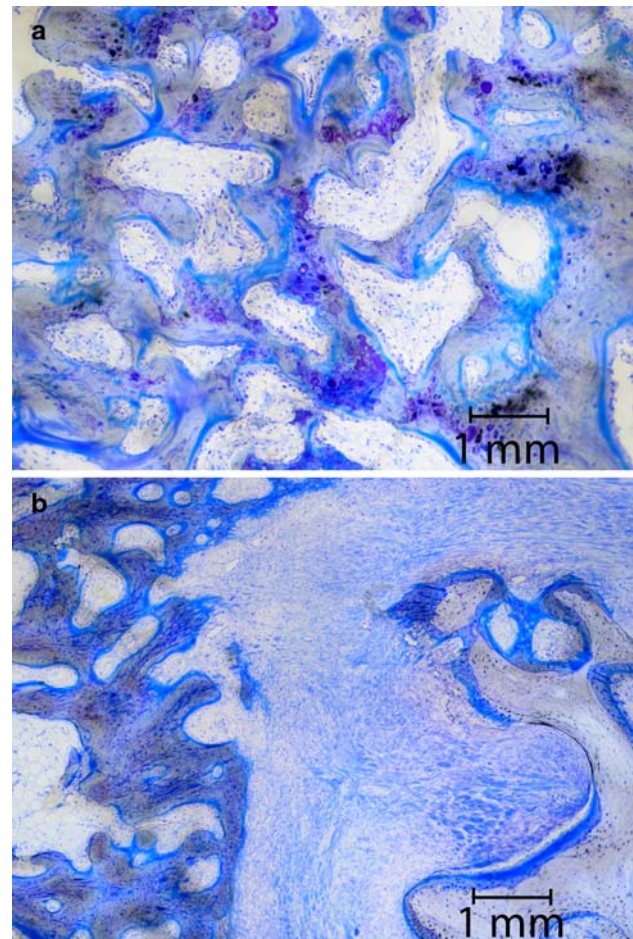The calculation of the patellar compression force in the stance phase of sheep showed that the force is

Fig. 6 Histological images of the bone-healing area in the osteotomy gap (magnification 20 times); **a** woven bone healing under 0.3 mm movement, **b** remaining connective tissue under 1 mm movement

approximately 1,200 N, which is about double the force necessary to achieve a deflection of 1 mm. The in vitro loading test showed that 575 N compression forces are high enough to cause a reversible deflection of 1 mm. This was confirmed by the X-ray under weight-bearing conditions, on which a closing of the osteotomy gap between the anterior osteotomy line and the implant could be observed.

Therefore a defined movement in the osteotomy gap at each loading cycle of the limb can be assumed. The movement in the osteotomy gap, however, will not be homogeneous along the whole osteotomy length. It will occur at the proximal part of the gap close to the implant but will be decrease in distal direction.

This can explain the different tissues observed at the proximal and distal part of the osteotomy gap with 1 mm movement in the proximal region. In this region of 1 mm movement, which corresponds to an interfragmentary strain of 33% fibrous cartilage is observed alongside beside some new bone formation. At the distal end of the partial osteotomy where the movement and interfragmentary

strain is much lower connective tissue can be seen. In the other sheep with 0.3 mm movement in the proximal gap, which corresponds to 10% interfragmentary strain, bony bridging of the whole osteotomy gap was observed. The newly formed bone had a trabecular structure. The original trabecular bone showed surfaces with new osteoid and intramembranous bone formation leading to a thickening of the trabeculae. In some areas of the woven bone, however, one could see structures on which remained endochondral ossification even though no fibrocartilaginous tissue was visible (Fig. 6a). It is possible that this bone formation was performed by former chondrocytes embedded in chondrocytic lacunae. It needs further studies with this new model to find out whether the newly formed bone is based on the endochondral like bone formation or a direct replacement of cartilage by bone based on an activity of chondrocytes [11, 13]. A biomechanical analysis of the tissue strain distribution in the gap could possibly elucidate the influence of the biomechanical environment on the local tissue differentiation.

Jarry and Uhthoff [9] performed the first experiments on the phases and histomorphology of metaphyseal fractures on rats. They manually created fractures of the distal femur, which resulted in a great variety of different fracture types ordered by criteria like non-displaced stable or displaced and unstable, the decision being made based on X-ray images and not on biomechanical measurements. Under "stable" conditions they observed very little or no callus formation on the periosteal side, which is in accordance with our results. Under "stable" conditions they found new bone formation starting 3 days after fracture and continuously replacing fibrous tissue in the fracture gap until the whole fracture gap was filled with new trabecular bone. No cartilage and consequently no enchondral bone was formed. This histological pattern observed was very similar to our results in the sheep with small interfragmentary movement (0.3 mm) and strain (10%). The sheep with 1 mm of interfragmentary movement correlates to clinical cases of metaphyseal fractures where some interfragmentary movement cannot be avoided and coupled with flexible fixation, a delay of healing can be observed [7].

Even though the interfragmentary movement was limited in one sheep to 1 mm this led to a delay in healing by the occurrence and persistence of fibrous cartilages. Similar histological images were found [9] for displaced and unstable transverse and oblique supracondylar and metaphysoepiphyseal fractures. This pilot study describes and characterizes a new metaphyseal bone-healing model. Additional studies have to show the reproducibility of the results found so far. If this can be confirmed this new model will be invaluable in studying the effect of various biomechanical conditions on fracture healing in normal and osteoporotic metaphyseal bone.

References

1. Bergmann G, Graichen F, Rohlmann A (1999) Hip joint forces in sheep. J Biomech 32:769–777
2. Claes LE, Wilke HJ, Augat P, Rübenacker S, Margevicius KJ (1995) Effect of dynamization on gap healing of diaphyseal fractures under external fixation. Clin Biomech (Bristol, Avon) 10:227–234
3. Claes LE, Augat P, Suger G, Wilke HJ (1997) Influence of size and stability of the osteotomy gap on the success of fracture healing. J Orthop Res 15:577–584
4. Claes LE, Heigele CA, Neidlinger-Wilke C, Kaspar D, Seidl W, Margevicius KJ, Augat P (1998) Effects of mechanical factors on the fracture healing process. Clin Orthop S355:S132–147
5. Claes LE, Eckert-Hübner K, Augat P (2002) The effect of mechanical stability on local vascularization and tissue differentiation in callus healing. J Orthop Res 20:1099–1105
6. Duda GN, Eckert-Hubner K, Sokiranski R, Kreutner A, Miller R, Claes L (1998) Analysis of inter-fragmentary movement as a function of musculoskeletal loading conditions in sheep. J Biomech 31:201–210
7. Duda GN, Sporrer S, Sollmann M, Hoffmann JE, Kassi JP, Khodadadyan C, Raschke M (2003) Interfragmentary movements in the early phase of healing in distraction and correction osteotomies stabilized with ring fixators. Langenbecks Arch Surg 387:433–440
8. Epari DR, Schell H, Bail HJ, Duda GN (2006) Instability prolongs the chondral phase during bone healing in sheep. Bone 38:864–870
9. Jarry L, Uhthoff HK (1971) Differences in healing of metaphyseal and diaphyseal fractures. Can J Surg 14:127–135
10. Kenwright J, Goodship AE (1989) Controlled mechanical stimulation in the treatment of tibial fractures. Clin Orthop Relat Res 241:36–47
11. Scammell BE, Roach HI (1996) A new role for the chondrocyte in fracture repair: endochondral ossification includes direct bone formation by former chondrocytes. J Bone Miner Res 11:737–745
12. Uhthoff HK, Rahn BA (1981) Healing patterns of metaphyseal fractures. Clin Orthop Relat Res 160:295–303
13. Yasui N, Sato M, Ochi T, Kimura T, Kawahata H, Kitamura Y, Nomura S (1997) Three modes of ossification during distraction osteogenesis in the rat. J Bone Joint Surg Br 79:824–830